QM-Cluster Model Study of the Guaiacol Hydrogen Atom Transfer and Oxygen Rebound with Cytochrome P450 Enzyme GcoA

Qianyi Cheng and Nathan J. DeYonker**

Department of Chemistry, University of Memphis, Memphis, TN 38152, U.S.A.

E-mail: qcheng1@memphis.edu*, ndyonker@memphis.edu*

Table S1: List of residues included in the optimized **1-10** and **1-15** QM cluster models. Total charge of models are +1 and 0, respectively.

RESIDUE	PROTONATED R GROUP?	SPECIES/RESIDUE CHARGE	TRIM N-SIDE	TRIM R-GROUP	TRIM C-SIDE
1-10					
V^{241}	N/A	0	H	-	-
Y^{242}	N/A	0	-	H	H
G^{245}	N/A	0	H	-	-
A^{246}	N/A	0	-	-	-
M^{247}	N/A	0	-	H	H
I^{292}	N/A	0	H	-	H
T^{296}	N/A	0	H	-	H
F^{349}	N/A	0	H	-	-
G^{350}	N/A	0	-	-	H
H^{354}	N	0	H	-	-
A^{355}	N/A	0	-	H	-
C^{356}	N/A	0	-	-	H
HEM^{501}	N/A	+3	N/A	N/A	N/A
$JZ3^{502}$	N/A	0	N/A	N/A	N/A
O^{904}	N/A	–2	N/A	N/A	N/A
1-15					
I^{81}	N/A	0	H	-	H
V^{241}	N/A	0	H	-	-
Y^{242}	N/A	0	-	H	H
L^{244}	N/A	0	H	H	-
G^{245}	N/A	0	-	-	-
A^{246}	N/A	0	-	-	-
M^{247}	N/A	0	-	H	H
E^{249}	N/A	–1	H	-	-
P^{250}	N/A	0	-	-	-
G^{251}	N/A	0	-	-	H
I^{292}	N/A	0	H	-	H
T^{296}	N/A	0	H	-	H
F^{349}	N/A	0	H	-	-
G^{350}	N/A	0	-	-	H
H^{354}	N	0	H	-	-
A^{355}	N/A	0	-	H	-
C^{356}	N/A	0	-	-	H
HEM^{501}	N/A	+3	N/A	N/A	N/A
$JZ3^{502}$	N/A	0	N/A	N/A	N/A
O^{904}	N/A	–2	N/A	N/A	N/A

Table S2: List of residues included in the optimized **2-10** and **2-15** QM cluster models. Total charge of both models are 0.

RESIDUE	PROTONATED R GROUP?	SPECIES/RESIDUE CHARGE	TRIM N-SIDE	TRIM R-GROUP	TRIM C-SIDE
2-10					
I^{81}	N/A	0	H	-	H
V^{241}	N/A	0	H	-	-
Y^{242}	N/A	0	-	H	H
L^{244}	N/A	0	H	H	-
G^{245}	N/A	0	-	-	-
A^{246}	N/A	0	-	-	-
M^{247}	N/A	0	-	H	H
I^{292}	N/A	0	H	-	H
T^{296}	N/A	0	H	-	H
C^{356}	N/A	0	H	-	H
HEM^{501}	N/A	+2	N/A	N/A	N/A
$JZ3^{502}$	N/A	0	N/A	N/A	N/A
O^{904}	N/A	–2	N/A	N/A	N/A
2-15					
F^{75}	N/A	0	H		H
I^{81}	N/A	0	H	-	H
F^{169}	N/A	0	H		H
V^{241}	N/A	0	H	-	-
Y^{242}	N/A	0	-	H	H
L^{244}	N/A	0	H	H	-
G^{245}	N/A	0	-	-	-
A^{246}	N/A	0	-	-	-
M^{247}	N/A	0	-	H	H
I^{292}	N/A	0	H	-	H
A^{295}	N/A	0	H	-	-
T^{296}	N/A	0	-	-	H
C^{356}	N/A	0	H	-	H
F^{395}	N/A	0	H		H
HEM^{501}	N/A	+2	N/A	N/A	N/A
$JZ3^{502}$	N/A	0	N/A	N/A	N/A
O^{904}	N/A	–2	N/A	N/A	N/A

Table S3: Bond distances of the reactants, transition states, and products of the two 10-residue and three 15-residue models in the Path A.

PATH A	r(Fe-O)	r[O-H(CH_2)]	r(H-CH_2)	r(O-CH_2)	r(Fe-S)
R1-10-A^4	1.63	2.06	1.09	3.12	2.53
TS1-10-A^4	1.69	1.25	1.30	2.55	2.41
P1-10-A^4	2.19	0.98	1.97	1.45	2.22
R1-10-A^2	1.63	2.02	1.09	3.07	2.53
TS1-10-A^2	1.69	1.25	1.30	2.55	2.41
P1-10-A^2	2.19	0.98	1.97	1.45	2.22
R1-15-A^4	1.63	2.08	1.09	3.11	2.54
TS1-15-A^4	1.75	1.19	1.35	2.53	2.45
P1-15-A^4	2.35	0.98	1.97	1.43	2.22
R1-15-A^2	1.63	2.08	1.09	3.11	2.54
TS1-15-A^2	1.75	1.19	1.35	2.53	2.45
P1-15-A^2	2.35	0.98	1.97	1.43	2.22
R2-10-A^4	1.63	2.18	1.09	3.22	2.50
TS2-10-A^4	1.69	1.29	1.28	2.56	2.43
P2-10-A^4	2.37	0.98	1.96	1.43	2.21
R2-10-A^2	1.63	2.11	1.09	3.18	2.52
TS2-10-A^2	1.70	1.27	1.29	2.55	2.43
P2-10-A^2	2.36	0.98	1.97	1.43	2.21
R2-15-A^4	1.63	2.09	1.09	3.17	2.56
TS2-15-A^4	1.69	1.31	1.25	2.55	2.40
P2-15-A^4	2.37	0.98	1.97	1.43	2.22
R2-15-A^2	1.63	2.09	1.09	3.17	2.56
TS2-15-A^2	1.74	1.19	1.33	2.51	2.35
P2-15-A^2	2.37	0.98	1.97	1.43	2.22
R3-15-A^4	1.63	2.12	1.09	3.18	2.58
TS3-15-A^4	1.74	1.30	1.26	2.56	2.41
P3-15-A^4	2.39	0.98	1.96	1.43	2.25
R3-15-A^2	1.62	2.13	1.09	3.19	2.57
TS3-15-A^2	1.71	1.29	1.27	2.56	2.45
P3-15-A^2	2.39	0.98	1.97	1.43	2.24

Table S4: Bond distances of the reactants, transition states, and products of the two 10-residue and three 15-residue models in the Path B.

PATH B	r(Fe-O)	r[O-H(CH_2)]	r(H-CH_2)	r(O-CH_2)	r(O-HO)	r(H-OC_6)	r(Fe-S)
R1-10-B^4	1.63	2.75	1.09	3.18	1.88	0.98	2.52
TS1-10-B^4	1.74	1.32	1.25	2.53	1.63	1.00	2.35
P1-10-B^4	2.34	0.98	1.97	1.45	1.80	0.98	2.21
R1-10-B^2	1.64	2.77	1.09	3.19	1.86	0.98	2.49
TS1-10-B^2	1.75	1.30	1.26	2.52	1.64	1.00	2.37
P1-10-B^2	2.22	0.98	1.97	1.46	1.82	0.98	2.20
R1-15-B^4	1.63	2.65	1.09	3.14	1.81	0.98	2.52
TS1-15-B^4	1.78	1.21	1.33	2.51	1.64	1.00	2.39
P1-15-B^4	2.35	0.98	1.98	1.45	1.76	0.98	2.21
R1-15-B^2	1.64	2.67	1.09	3.15	1.82	0.98	2.50
TS1-15-B^2	1.78	1.21	1.33	2.51	1.66	1.00	2.39
P1-15-B^2	2.35	0.98	1.98	1.45	1.76	0.98	2.21
R2-10-B^4	1.63	2.60	1.09	3.04	1.83	0.98	2.51
TS2-10-B^4	1.77	1.23	1.32	2.51	1.67	0.99	2.35
P2-10-B^4	2.37	0.99	1.98	1.45	1.76	0.98	2.20
R2-10-B^2	1.64	2.61	1.09	3.05	1.83	0.98	2.49
TS2-10-B^2	1.75	1.36	1.22	2.54	1.61	1.00	2.32
P2-10-B^2	2.37	0.99	1.98	1.45	1.76	0.98	2.21
R2-15-B^4	1.63	2.86	1.09	3.17	1.77	0.99	2.53
TS2-15-B^4	1.78	1.22	1.32	2.51	1.61	1.00	2.44
P2-15-B^4	2.38	0.99	1.98	1.45	1.77	0.98	2.21
R2-15-B^2	1.63	2.72	1.09	3.17	1.71	0.99	2.54
TS2-15-B^2	1.76	1.33	1.24	2.53	1.61	1.00	2.34
P2-15-B^2	2.38	0.99	1.98	1.44	1.78	0.98	2.21
R3-15-B^4	1.63	2.72	1.09	3.15	1.82	0.98	2.58
TS3-15-B^4	1.78	1.22	1.32	2.50	1.62	1.00	2.48
P3-15-B^4	2.40	0.98	1.98	1.45	1.76	0.98	2.23
R3-15-B^2	1.63	2.74	1.09	3.25	1.84	0.98	2.57
TS3-15-B^2	1.76	1.33	1.24	2.53	1.62	1.00	2.37
P3-15-B^2	2.38	0.99	1.98	1.45	1.71	0.98	2.23

Table S5. Reaction free energies of the **1-10** models and **1-15** models. The doublet spin state of 10-residue model in Path A is the lowest energy reactant (in red/bold); the quartet spin state of the 15-residue model in Path A is the lowest energy reactant (in red/bold). Gibbs free energies are given in kcal mol^{-1}.

	10 Residue Model				15 Residue Model		
RUN 1	Reactant	TS	Product	**RUN 1**	Reactant	TS	Product
10-A^4	0.88	10.32	-53.57	**15-A^4**	**0.00**	15.90	-56.08
10-A^2	**0.00**	10.60	-52.93	**15-A^2**	0.40	16.07	-55.68
10-B^4	5.16	19.96	-49.68	**15-B^4**	6.49	22.48	-46.06
10-B^2	13.17	20.01	-45.14	**15-B^2**	15.64	22.40	-45.64

Table S6. Reaction free energies of the **2-10** models and **2-15** models. The quartet spin state of 10-residue model in Path A is the lowest energy reactant (in red/bold); the quartet spin state of the 15-residue model in Path B is the lowest energy reactant (in red/bold). Gibbs free energies are given in kcal mol^{-1}.

	10 Residue Model				15 Residue Model		
RUN 2	Reactant	TS	Product	**RUN 2**	Reactant	TS	Product
10-A^4	**0.00**	12.61	-57.73	**15-A^4**	**0.00**	12.66	-56.96
10-A^2	1.24	13.34	-56.54	**15-A^2**	0.43	13.69	-56.50
10-B^4	3.86	19.30	-52.20	**15-B^4**	8.22	24.20	-47.14
10-B^2	12.84	18.74	-51.74	**15-B^2**	14.57	28.18	-42.12

Table S7. Reaction free energies of the **3-15** models. The quartet spin state model in Path A is the lowest energy reactant (in red/bold). Gibbs free energies are given in kcal mol^{-1}.

	15 Residue Model		
RUN 3	Reactant	TS	Product
15-A^4	**0.00**	13.52	-56.66
15-A^2	0.72	13.43	-55.83
15-B^4	9.22	24.41	-47.62
15-B^2	18.60	31.13	-42.37

Table S8: Absolute (free) energies (in au) of optimized geometries of the GcoA model with guaiacol in path A and B.

PATH A	E	E+ZPE	G	PATH B	E	E+ZPE	G
R1-10-A^4	-5385.381056	-5383.571555	-5383.717556	**R1-10-B^4**	-5385.370898	-5383.562466	-5383.710747
TS1-10-A^4	-5385.359668	-5383.555370	-5383.702514	**TS1-10-B^4**	-5385.343991	-5383.540386	-5383.687149
P1-10-A^4	-5385.472362	-5383.659367	-5383.804327	**P1-10-B^4**	-5385.467700	-5383.652800	-5383.798142
R1-10-A^2	-5385.382822	-5383.573696	-5383.718965	**R1-10-B^2**	-5385.357001	-5383.549216	-5383.697973
TS1-10-A^2	-5385.359701	-5383.555571	-5383.702078	**TS1-10-B^2**	-5385.344298	-5383.541228	-5383.687085
P1-10-A^2	-5385.472006	-5383.659099	-5383.803320	**P1-10-B^2**	-5385.459358	-5383.646317	-5383.790905
R1-15-A^4	-6707.507325	-6705.185920	-6705.360426	**R1-15-B^4**	-6707.497509	-6705.176804	-6705.350076
TS1-15-A^4	-6707.476618	-6705.163036	-6705.335084	**TS1-15-B^4**	-6707.466705	-6705.152583	-6705.324598
P1-15-A^4	-6707.607573	-6705.281376	-6705.449803	**P1-15-B^4**	-6707.589345	-6705.263871	-6705.433833
R1-15-A^2	-6705.185918	-6705.359794	-6705.185918	**R1-15-B^2**	-6707.483084	-6705.162795	-6705.335510
TS1-15-A^2	-6707.477353	-6705.163627	-6705.334818	**TS1-15-B^2**	-6707.466854	-6705.153334	-6705.324723
P1-15-A^2	-6707.607577	-6705.281373	-6705.449151	**P1-15-B^2**	-6707.589348	-6705.263865	-6705.433156
R2-10-A^4	-4591.502028	-4589.884348	-4590.016785	**R2-10-B^4**	-4591.493183	-4589.877559	-4590.010635
TS2-10-A^4	-4591.474535	-4589.863939	-4589.996693	**TS2-10-B^4**	-4591.462058	-4589.853007	-4589.986027
P2-10-A^4	-4591.600308	-4589.978614	-4590.108779	**P2-10-B^4**	-4591.587300	-4589.967434	-4590.099970
R2-10-A^2	-4591.495786	-4589.881109	-4590.014805	**R2-10-B^2**	-4591.479087	-4589.863884	-4589.996319
TS2-10-A^2	-4591.471073	-4589.862550	-4589.995525	**TS2-10-B^2**	-4591.463756	-4589.854121	-4589.986913
P2-10-A^2	-4591.596823	-4589.976915	-4590.106882	**P2-10-B^2**	-4591.587271	-4589.967393	-4590.099235
R2-15-A^4	-5928.643296	-5926.374022	-5926.534630	**R2-15-B^4**	-5928.628086	-5926.359945	-5926.521534
TS2-15-A^4	-5928.620178	-5926.356353	-5926.514452	**TS2-15-B^4**	-5928.600044	-5926.338202	-5926.496067
P2-15-A^4	-5928.743981	-5926.469852	-5926.625402	**P2-15-B^4**	-5928.726092	-5926.452643	-5926.609748
R2-15-A^2	-5928.643320	-5926.374072	-5926.533945	**R2-15-B^2**	-5928.618408	-5926.350788	-5926.511419
TS2-15-A^2	-5928.618614	-5926.355399	-5926.512812	**TS2-15-B^2**	-5928.591874	-5926.330577	-5926.489716
P2-15-A^2	-5928.743966	-5926.469808	-5926.624674	**P2-15-B^2**	-5928.715684	-5926.443702	-5926.601758
R3-15-A^4	-5928.640829	-5926.376562	-5926.534976	**R3-15-B^4**	-5928.623358	-5926.359801	-5926.520282
TS3-15-A^4	-5928.616035	-5926.357727	-5926.513436	**TS3-15-B^4**	-5928.595884	-5926.339050	-5926.496073
P3-15-A^4	-5928.739093	-5926.471266	-5926.625273	**P3-15-B^4**	-5928.722085	-5926.454676	-5926.610870
R3-15-A^2	-5928.640633	-5926.375857	-5926.533832	**R3-15-B^2**	-5928.606015	-5926.344766	-5926.505335
TS3-15-A^2	-5928.614766	-5926.357662	-5926.513573	**TS3-15-B^2**	-5928.581173	-5926.326184	-5926.485371
P3-15-A^2	-5928.738894	-5926.470663	-5926.623951	**P3-15-B^2**	-5928.712260	-5926.446172	-5926.602490

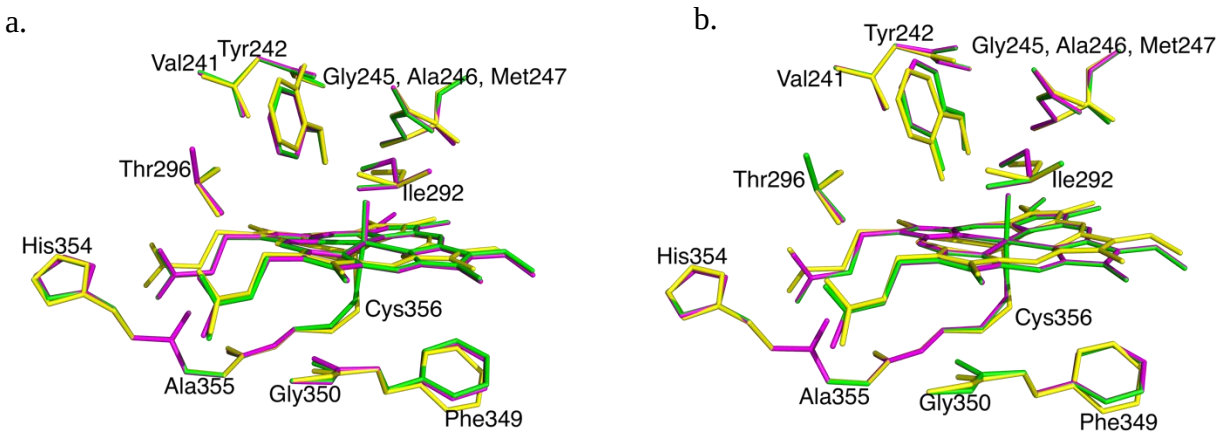

Figure S1. Aligned optimized reactants of the **1-10** models in Path A (a) and Path B (b) doublet state (green, **R1-10-A^2** and **R1-10-B^2**), quartet state (magenta, **R1-10-A^4** and **R1-10-B^4**) and 10-residue model from the X-ray crystal structure (yellow, Tmp1-10-A and Tmp1-10-B) with two different guaiacol orientations.

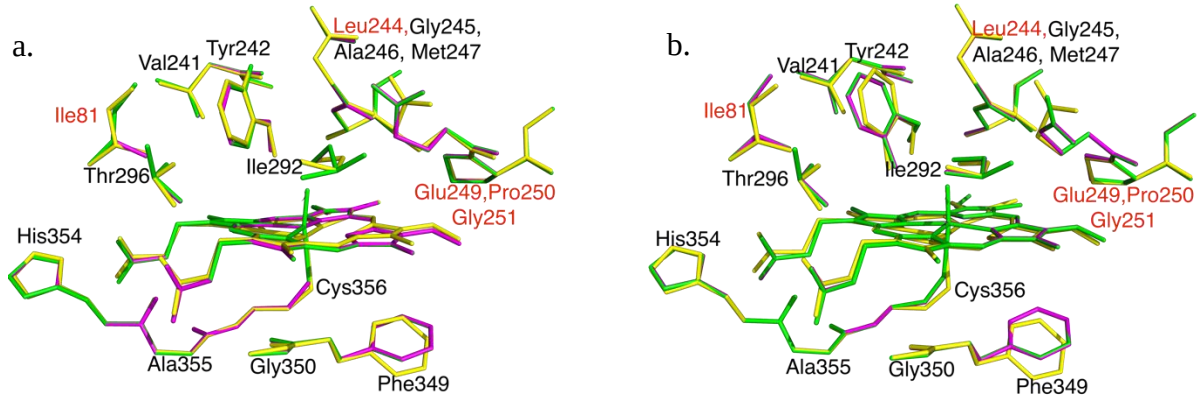

Figure S2. Aligned optimized reactants of the **1-15** models in Path A (a) and Path B (b), doublet state (green, **R1-15-A^2** and **R1-15-B^2**), quartet state (magenta, **R1-15-A^4** and **R1-15-B^4**) and 15-residue model from the X-ray crystal structure (yellow, Tmp1-15-A and Tmp1-15-B) with two different guaiacol orientations. The residues in red are the additional ones compared to the **1-10** model.

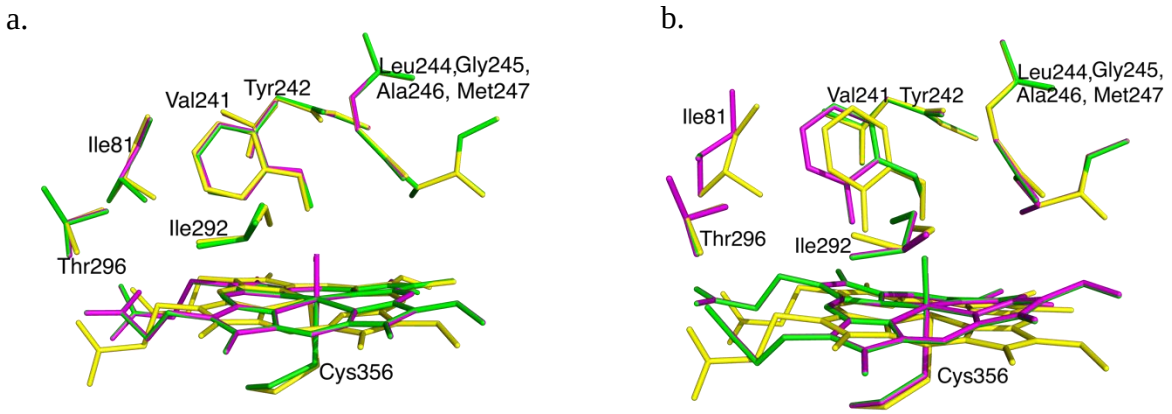

Figure S3. Aligned optimized reactants of the **2-10** models in Path A (a) and Path B (b), doublet state (green, **R2-10-A**^{2} and **R2-10-B**^{2}), quartet state (magenta, **R2-10-A**^{4} and **R2-10-B**^{4}) and 10-residue model from the X-ray crystal structure (yellow, Tmp2-10-A and Tmp2-10-B) with two different guaiacol orientations.

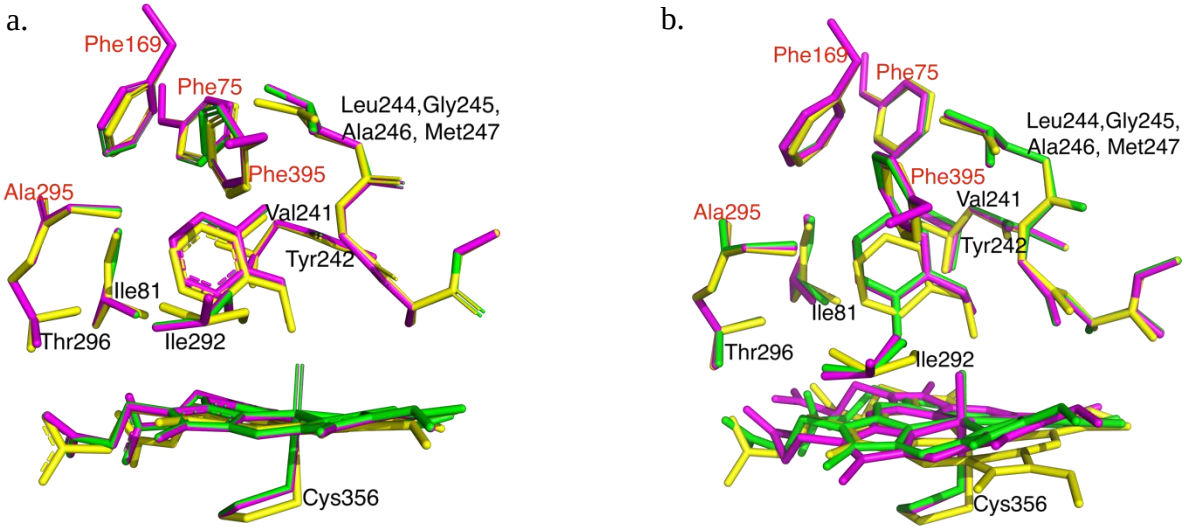

Figure S4. Aligned optimized reactants of the **2-15** models in Path A (a) and Path B (b), doublet state (green, **R2-15-A**^{2} and **R2-15-B**^{2}), quartet state (magenta, **R2-15-A**^{4} and R**2-15-B**^{4}) and 15-residue model from the X-ray crystal structure (yellow, Tmp2-15-A and Tmp2-15-B) with two different guaiacol orientations. The residues in red are the additional ones compared to the **2-10** model.

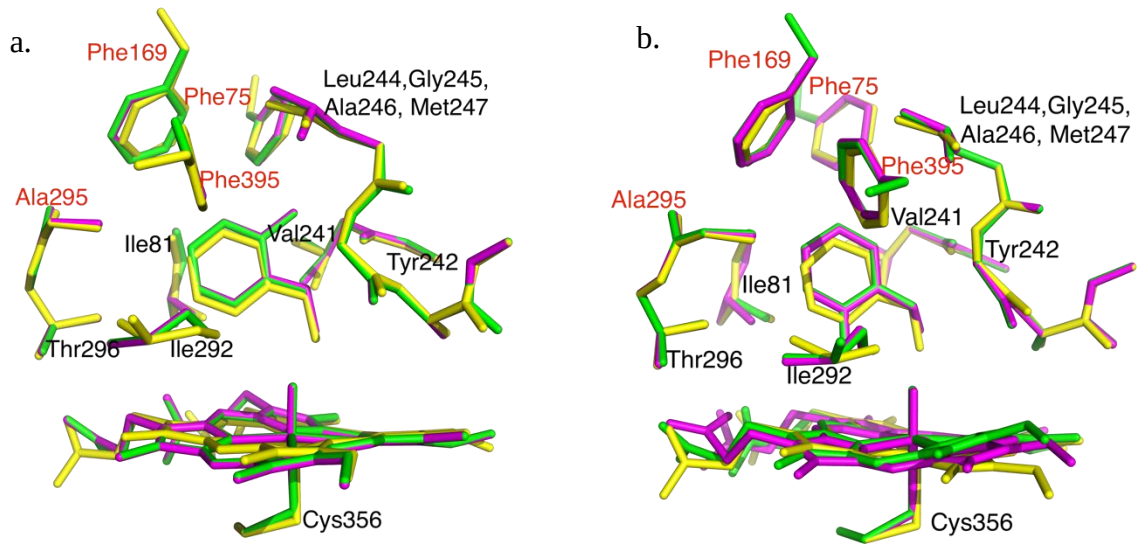

Figure S5. Aligned optimized reactants of the **3-15** models in Path A (a) and Path B (b), doublet state (green, **R3-15-A^2** and **R3-15-B^2**), quartet state (magenta, **R3-15-A^4** and **R3-15-B^4**) and 15-residue model from the X-ray crystal structure (yellow, Tmp2-15-A and Tmp2-15-B) with two different guaiacol orientations.

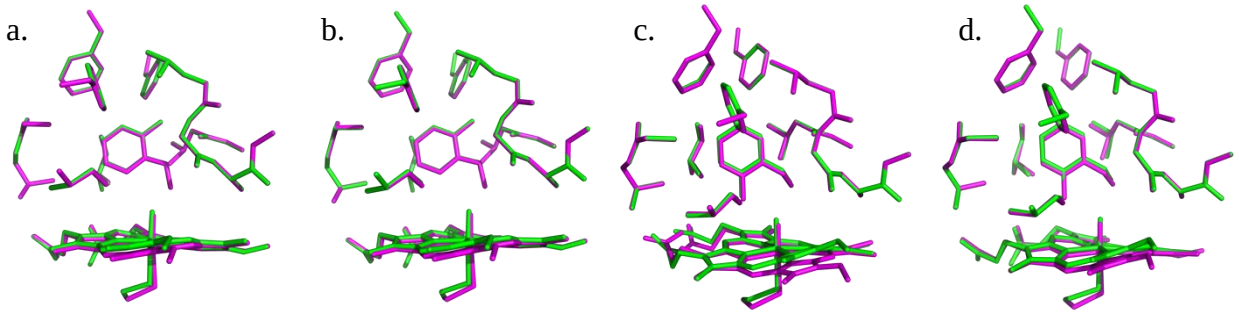

Figure S6. Aligned optimized reactants of the R2-15 (green) and R3-15 (magenta) in Path A and B and doublet and quartet spin state, (a) R-A^2, (b) R-A^4, (c) R-B^2, (d) R-B^4.